ISSN 0021-3640, JETP Letters, 2023, Vol. 117, No. 12, pp. 923–931. © Pleiades Publishing, Inc., 2023.
Russian Text © The Author(s), 2023, published in Pis'ma v Zhurnal Eksperimental'noi i Teoreticheskoi Fiziki, 2023, Vol. 117, No. 12, pp. 919–928.

CONDENSED MATTER

Photoinduced Enhancement of the Excitonic Order in Strongly Correlated Electron Systems with the Spin Crossover

Yu. S. Orlov[a,b,*], S. V. Nikolaev[a,b], and S. G. Ovchinnikov[a,b]

[a] *Siberian Federal University, Krasnoyarsk, 660041 Russia*

[b] *Kirensky Institute of Physics, Federal Research Center KSC, Siberian Branch, Russian Academy of Sciences, Krasnoyarsk, 660036 Russia*

** e-mail: jso.krasn@mail.ru*

Received May 12, 2023; revised May 12, 2023; accepted May 18, 2023

A new mechanism of the photoinduced enhancement of the excitonic order in strongly correlated electron systems with the spin crossover through the generation of a massive mode in the spectrum of collective excitations is demonstrated.

DOI: 10.1134/S0021364023601513

1. INTRODUCTION

The study of the nonequilibrium dynamics of strongly correlated systems can provide a new insight into their properties and new ways to control various ordered states that arise as a result of phase transitions. For example, the nonequilibrium properties of superconductors are now widely studied. Both the light-induced enhancement of superconductivity [1–3] and the observation of the Higgs mode [4–6] were reported. Recently, a related family of ordered states, excitonic insulators, has also attracted a wide interest [7–12]. Among the theoretical works in this direction, we would like to single out work [13], where the authors demonstrated a new mechanism for the photoinduced enhancement of the excitonic order in the framework of a two-band model of spinless fermions coupled to phonons. According to [13], the combination of photoexcitation and the symmetry reduction of the Hamiltonian can ensure a new strategy for the enhancement of the superconducting order parameter in superconductors. Some similarity between the exciton condensate state and the superconducting one makes it promising to study the nonequilibrium characteristics of such systems.

The theoretical and experimental studies of the excitonic order in strongly correlated systems with the spin crossover have so far been focused on their equilibrium properties [14–24]. The study of nonequilibrium characteristics has only just started. In view of the recent development of the pump–probe spectroscopy with a high time resolution, the possibility of spin crossover under the effect of femtosecond laser pulses becomes a topical issue [25, 26].

In contrast to conventional excitonic insulators, where the Coulomb interaction is responsible for electron–hole pairing and for the formation of excitons, in the case of the systems with spin crossover, the excitonic order is due to intersite electron hopping. Nevertheless, the mechanism of photoinduced enhancement proposed in [13] can also be viable in this case. We demonstrate that the photoinduced enhancement of the exciton condensate is possible in strongly correlated systems with the spin crossover, and such effect is not related to the transition to a metastable or any excited state. The scientific novelty of this work is the determination of the cooperative effects arising owing to interatomic exciton and electron–phonon interactions under nonequilibrium conditions.

2. EFFECTIVE HAMILTONIAN

The minimal model describing strongly correlated electron systems with the spin crossover is the two-band Hubbard–Kanamori model. The Hamiltonian of the model can be written as

$$\hat{H} = \hat{H}_\Delta + \hat{H}_t + \hat{H}_{\text{Coulomb}}. \quad (1)$$

Here,

$$\hat{H}_\Delta = \varepsilon_1 \sum_{i,\gamma} c^\dagger_{1i\gamma} c_{1i\gamma} + \varepsilon_2 \sum_{i,\gamma} c^\dagger_{2i\gamma} c_{2i\gamma} \quad (2)$$

includes the single-site energy of electrons occupying single-particle states corresponding to the energy levels ε_1 and $\varepsilon_2 = \varepsilon_1 + \Delta$, where Δ is the electron energy in the crystal field (for the sake of convenience, we can

set $\varepsilon_1 = 0$), i enumerates lattice sites, and $\gamma = \pm 1/2$ is the electron spin projection;

$$\hat{H}_t = t_{11}\sum_{\langle i,j\rangle,\gamma} c^{\dagger}_{1i\gamma}c_{1j\gamma} + t_{22}\sum_{\langle i,j\rangle,\gamma} c^{\dagger}_{2i\gamma}c_{2j\gamma} + t_{12}\sum_{\langle i,j\rangle,\gamma}\left(c^{\dagger}_{2i\gamma}c_{1j\gamma} + c^{\dagger}_{1i\gamma}c_{2j\gamma}\right), \quad (3)$$

where $t_{\lambda\lambda'}$ ($\lambda,\lambda' = 1,2$ are orbital indices) are the hopping integrals describing electron hopping between the nearest neighbor sites in the crystal lattice (the sites are characterized by energy levels ε_1 and ε_2); and

$$\begin{aligned}\hat{H}_{\text{Coulomb}} &= U\sum_{\lambda,i} c^{\dagger}_{\lambda i\uparrow}c^{\dagger}_{\lambda i\downarrow}c_{\lambda i\uparrow}c_{\lambda i\downarrow} \\ &+ V\sum_{\lambda\neq\lambda',i} c^{\dagger}_{\lambda i\uparrow}c^{\dagger}_{\lambda' i\downarrow}c_{\lambda i\uparrow}c_{\lambda' i\downarrow} \\ &+ V\sum_{\lambda>\lambda',i,\gamma} c^{\dagger}_{\lambda i\gamma}c^{\dagger}_{\lambda' i\gamma}c_{\lambda i\gamma}c_{\lambda' i\gamma} \\ &+ J_{\text{H}}\sum_{\lambda>\lambda',i,\gamma} c^{\dagger}_{\lambda i\gamma}c^{\dagger}_{\lambda' i\gamma}c_{\lambda' i\gamma}c_{\lambda i\gamma} \\ &+ J_{\text{H}}\sum_{\lambda\neq\lambda',i} c^{\dagger}_{\lambda i\uparrow}c^{\dagger}_{\lambda' i\downarrow}c_{\lambda' i\uparrow}c_{\lambda i\downarrow} \\ &+ J'_{\text{H}}\sum_{\lambda\neq\lambda',i} c^{\dagger}_{\lambda i\uparrow}c^{\dagger}_{\lambda i\downarrow}c_{\lambda' i\uparrow}c_{\lambda' i\downarrow},\end{aligned} \quad (4)$$

where U and V are the diagonal and off-diagonal matrix elements in the orbital indices, respectively, and J_{H} and J'_{H} are the parameters of Hund's exchange interactions, represents the onsite Coulomb interaction energy of electrons in the Kanamori approximation [27].

An important feature of such two-orbital model is that different localized multielectron (two-particle) states (terms), which are characterized by the spin values $S = 0,1$ and by the crossover between them with an increase in Δ, can be formed in the case of half-filling ($N_e = 2$ is the average number of electrons per crystal lattice site) and in the zeroth approximation in terms of hopping integrals ($t_{\lambda\lambda'} = 0$). In the region $\Delta < \Delta_C = \sqrt{(U - V + J_{\text{H}})^2 + J'^2_{\text{H}}}$, the ground state is the triplet HS ($S = 1$) state $|\sigma\rangle$ with the energy E_{HS}, which is triply degenerate in the spin projection $\sigma = 0,\pm 1$:

$$|\sigma\rangle = \begin{cases} a^{\dagger}_{1\uparrow}a^{\dagger}_{2\uparrow}|0\rangle, & \sigma = +1, \\ \frac{1}{\sqrt{2}}\left(a^{\dagger}_{1\uparrow}a^{\dagger}_{2\downarrow}|0\rangle + a^{\dagger}_{1\downarrow}a^{\dagger}_{2\uparrow}|0\rangle\right), & \sigma = 0, \\ a^{\dagger}_{1\downarrow}a^{\dagger}_{2\downarrow}|0\rangle, & \sigma = -1. \end{cases}$$

At $\Delta > \Delta_C$, the ground state is the singlet LS ($S = 0$) state $|s\rangle = C_1(\Delta)a^{\dagger}_{1\uparrow}a^{\dagger}_{1\downarrow}|0\rangle - C_2(\Delta)a^{\dagger}_{2\uparrow}a^{\dagger}_{2\downarrow}|0\rangle$ with the energy E_{LS}, where $C_1(\Delta) = \sqrt{1 - C_2^2(\Delta)}$ and $C_2(\Delta) = x/2\left(1 + x + \sqrt{1+x}\right)$ are the normalization coefficients ($x = J'^2_{\text{H}}/\Delta^2$).

To derive the effective Hamiltonian, it is convenient to use the Hubbard X operators $X^{p,q} = |p\rangle\langle q|$ [28], which are expressed in terms of the eigenstates of the Hamiltonian $\hat{H}_{\Delta} + \hat{H}_{\text{Coulomb}}$

$$\left(\hat{H}_{\Delta} + \hat{H}_{\text{Coulomb}}\right)|p\rangle = E_p|p\rangle \quad (5)$$

with different numbers of electrons $N_e = 0$–4. Since the Hubbard operators form a linearly independent basis, any local operator can be expressed in terms of a linear combination of the X operators. In particular, the single-electron annihilation (creation) operator is represented in the form

$$c_{\lambda i\gamma} = \sum_{pq}|p\rangle\langle p|c_{\lambda i\gamma}|q\rangle\langle q| = \sum_{pq}\chi_{\lambda\gamma}(p,q)X_i^{p,q}. \quad (6)$$

Since the number of various pairs of states (p,q) differing by unity is finite, they can be enumerated. Each pair can be matched with the number l [29] having the meaning of the band index of local Fermi quasiparticles. Then, $c_{i\lambda\gamma} = \sum_l \chi_{\lambda\gamma}(l)X_i^l$ and $c^{\dagger}_{i\lambda\gamma} = \sum_l \chi^*_{\lambda\gamma}(l)X_i^{l\dagger}$. Using Eq. (6), the anomalous averages $\left\langle a^{\dagger}_{2f\gamma}a_{1f\gamma}\right\rangle$ (without spin flip) and $\left\langle a^{\dagger}_{2f\bar{\gamma}}a_{1f\gamma}\right\rangle$ (with spin flip, $\bar{\gamma} = -\gamma$) can be represented in the form

$$\left\langle c^{\dagger}_{2f\gamma}c_{1f\gamma}\right\rangle \approx -\gamma\sqrt{2}\left(C_2\left\langle X_f^{s,0}\right\rangle + C_1\left\langle X_f^{0,s}\right\rangle\right), \quad (7)$$

$$\begin{aligned}\left\langle c^{\dagger}_{2f\bar{\gamma}}c_{1f\gamma}\right\rangle &\approx 2\gamma\left(\gamma - \frac{1}{2}\right)\left(C_2\left\langle X_f^{s,-1}\right\rangle + C_1\left\langle X_f^{-1,s}\right\rangle\right) \\ &- 2\gamma\left(\gamma + \frac{1}{2}\right)\left(C_2\left\langle X_f^{s,+1}\right\rangle + C_1\left\langle X_f^{+1,s}\right\rangle\right).\end{aligned} \quad (8)$$

Here, we omit the averages of X operators built on the states with the numbers of electrons smaller and larger than two. We consider the case of half filling (two-particle states) with a fixed number of electrons per site of the crystal lattice (the homopolar model of solid); therefore, the contribution of such averages is negligibly small.

As seen in Eqs. (7) and (8), the excitonic pairing is described by nonzero averages of singlet–triplet excitations. Here and below, the angle brackets $\langle\ldots\rangle$ denote quantum statistical averages. Nonzero averages $\left\langle X_i^{\sigma,s}\right\rangle = \left\langle\left(X_i^{s,\sigma}\right)^{\dagger}\right\rangle = \left\langle X_i^{s,\sigma}\right\rangle^*$ correspond to the quantum entanglement of the LS and HS states in the absence of spin–orbit coupling. The Hamiltonian (1) in the representation of Hubbard X operators has the form

$$\hat{H} = \sum_{i,p}E_pX_i^{p,p} + \sum_{\langle i,j\rangle}\sum_{l,k}t^{lk}X_i^{l\dagger}X_j^k. \quad (9)$$

Here, E_p is the energy of multielectron terms and $t^{lk} = \sum_{\lambda,\lambda',\gamma} t_{\lambda\lambda'}\chi^*_{\lambda\gamma}(l)\chi_{\lambda'\gamma}(k)$ are the renormalized hopping parameters.

Using the Hamiltonian (9) as an initial one, we can obtain the effective Hamiltonian excluding interband hops. For this, we employ the projection operator method developed in [30] for the Hubbard model and in [31] for the p–d model (see also [14, 15]). The effective Hamiltonian has the form

$$\hat{H}_{\text{eff}} = \hat{H}_S + \hat{H}_{n_{\text{LS}}n_{\text{LS}}} + \hat{H}_{\text{ex}}. \quad (10)$$

Here, the first term is the Heisenberg Hamiltonian containing the interatomic exchange interaction

$$\hat{H}_S = \frac{1}{2}J\sum_{\langle i,j\rangle}\left(\hat{\mathbf{S}}_i\cdot\hat{\mathbf{S}}_j - \frac{1}{4}\hat{n}_i\hat{n}_j\right). \quad (11)$$

Here, $J = \left(t_{11}^2 + 2t_{12}^2 + t_{22}^2\right)/\Omega_g$ is the magnitude of the interatomic exchange interaction, where Ω_g is the energy of charge transfer between the centers of the upper and lower Hubbard subbands [30, 31]; $\hat{\mathbf{S}}_i$ is the spin-1 operator, which can be specified by the components $\hat{S}_i^+ = \sqrt{2}\left(X_i^{+1,0} + X_i^{0,-1}\right)$, $\hat{S}_i^- = \sqrt{2}\left(X_i^{0,+1} + X_i^{-1,0}\right)$, and $\hat{S}_i^z = X_i^{+1,+1} - X_i^{-1,-1}$ [32]; and $\hat{n}_i = 2\left(X_i^{s,s} + \sum_\sigma X_i^{\sigma,\sigma}\right) = 2\left(\hat{n}_i^{\text{LS}} + \hat{n}_i^{\text{HS}}\right)$ is the operator of the number of particles at the ith site ($\hat{n}_i^{\text{LS(HS)}}$ is the occupation number operator for the LS (HS) state). Using the condition of completeness $X^{s,s} + \sum_\sigma X^{\sigma,\sigma} = 1$, one can show that $\langle\hat{n}_i\rangle = 2\left(\left\langle\hat{n}_i^{\text{LS}}\right\rangle + \left\langle\hat{n}_i^{\text{HS}}\right\rangle\right) = 2\left(n_{\text{LS}} + n_{\text{HS}}\right) = 2$, where $n_{\text{LS(HS)}}$ ($n_{\text{LS}} + n_{\text{HS}} = 1$).

The second term in Eq. (10)

$$\hat{H}_{n_{\text{LS}}n_{\text{LS}}} = \frac{1}{2}\tilde{J}\sum_{\langle i,j\rangle} X_i^{s,s}X_j^{s,s} \quad (12)$$

describes the density–density interaction between low-spin states, where $\tilde{J} = \left[1 - \left(2C_1C_2\right)^2\right]\times\left(t_{11}^2 - 2t_{12}^2 + t_{22}^2\right)/\Omega_g$.

The third term in Eq. (10)

$$\hat{H}_{\text{ex}} = -\frac{\varepsilon_{\text{S}}}{2}\sum_i\left(X_i^{s,s} - \sum_{\sigma=-S}^{+S}X_i^{\sigma,\sigma}\right) + \sum_\sigma\sum_{\langle i,j\rangle}\left[\frac{1}{2}J'_{\text{ex}}\left(X_i^{\sigma,s}X_j^{s,\sigma} + X_i^{s,\sigma}X_j^{\sigma,s}\right) - \frac{1}{2}J''_{\text{ex}}(-1)^{|\sigma|}\left(X_i^{\sigma,s}X_j^{\bar{\sigma},s} + X_i^{s,\sigma}X_j^{s,\bar{\sigma}}\right)\right], \quad (13)$$

where $\varepsilon_{\text{S}} = E_{\text{HS}} - E_{\text{LS}}$ is the spin gap and $\bar{\sigma} = -\sigma$, includes the interatomic hopping of excitons with the amplitude $J'_{\text{ex}} = 2C_1C_2\left(t_{11}t_{22} - t_{12}^2\right)/\Omega_g$ and the creation/annihilation of biexcitons at neighboring sites with the amplitude $J''_{\text{ex}} = \left(t_{11}t_{22} - t_{12}^2\right)/\Omega_g$ taking into account the energy of electronic configurations of the LS and HS states. In the absence of all cooperative interactions, the ground state in the cases of negative and positive spin gaps is the HS and LS states, respectively. In Eq. (13), the Hubbard operators $X_i^{\sigma,s}$ and $X_i^{s,\sigma}$ describe Bose excitations (excitons) at the ith site from the low-spin singlet state $|s\rangle$ to the high-spin triplet one $|\sigma\rangle$ with the spin projection $\sigma = 0, \pm 1$ and back, respectively. The first term in square brackets in Eq. (13) describes the dispersion of excitons caused by interatomic hops; this dispersion was considered in [33]. The second term in square brackets in Eq. (13) involves the creation and annihilation of biexcitons at the neighboring ith and jth sites of the lattice, which immediately complicates the dispersion of excitons compared to the conventional dispersion in the tight binding method [33]. Near the spin crossover, $C_1 \approx 1$ and $C_2 \approx 0$; consequently, $J'_{\text{ex}} \approx 0$. Under these conditions, biexcitons play the dominant role in the formation of dispersion of excitons. The Hamiltonian (13) describes the kinetic exciton–exciton interaction [34] in the representation of Hubbard X operators.

If we introduce the notation $\hat{d}_x = \frac{1}{\sqrt{2}}\left(-\hat{d}_+ + \hat{d}_-\right)$, $\hat{d}_y = \frac{1}{\sqrt{2}i}\left(\hat{d}_+ + \hat{d}_-\right)$, and $\hat{d}_z = \hat{d}_0$ [20], where $\hat{d}_+ = X^{s,+}$, $\hat{d}_- = X^{s,-}$, and $\hat{d}_0 = X^{s,0}$, then the last term in (13) can be represented in the form

$$\frac{J'_{\text{ex}}}{2}\sum_{\langle i,j\rangle}\left(\hat{\mathbf{d}}_i^\dagger\cdot\hat{\mathbf{d}}_j + \hat{\mathbf{d}}_i\cdot\hat{\mathbf{d}}_j^\dagger\right) - \frac{J''_{\text{ex}}}{2}\sum_{\langle i,j\rangle}\left(\hat{\mathbf{d}}_i^\dagger\cdot\hat{\mathbf{d}}_j^\dagger + \hat{\mathbf{d}}_i\cdot\hat{\mathbf{d}}_j\right). \quad (14)$$

The vector $\hat{\mathbf{d}} = \left(\hat{d}_x, \hat{d}_y, \hat{d}_z\right)$ corresponds to the so-called $\mathbf{d}$ vector in the triplet superconductivity theory.

In [35], we analyzed the features of the formation of exciton Bose condensate, which corresponds to the condensation of local (at a crystal lattice site) magnetic excitons (small-radius excitons), in strongly correlated systems near the spin crossover, which is described by the Hamiltonian (13) and by the excitonic order parameter $\Delta_{\text{ex}}^\sigma = \left\langle X_i^{s,\sigma}\right\rangle$. In [35], the coexistence of antiferromagnetism and exciton condensate and the formation of long-range antiferromagnetic order due to the excitonic order even in the absence of interatomic exchange interaction (11) were demonstrated.

In what follows, for convenience, all quantities will be measured in units of the exchange interaction $J =$ 28 K [36], even when this interaction is not taken into account.

Taking into account the electron–phonon interaction, we have

$$\hat{H} = \hat{H}_{\text{eff}} + \hat{H}_{1\text{ph}} + \hat{H}_{2\text{ph}}, \tag{15}$$

where

$$\begin{aligned}\hat{H}_{1\text{ph}} &= \omega_{0(1)}\sum_i\left(a_i^\dagger a_i + \frac{1}{2}\right)\\ &+ g_1\sum_i\left(a_i + a_i^\dagger\right)\left(X_i^{s,s} - \sum_{\sigma=-1}^{+1}X_i^{\sigma,\sigma}\right)\end{aligned} \tag{16}$$

contains the diagonal electron–phonon interaction and describes the isotropic compression/expansion of cation–anion octahedra (the *a* type phonon mode corresponds to the breathing mode for a metal–ligand octahedron) and

$$\begin{aligned}\hat{H}_{2\text{ph}} &= \omega_{0(2)}\sum_i\sum_{\sigma=-1}^{+1}\left(b_{i,\sigma}^\dagger b_{i,\sigma} + \frac{1}{2}\right)\\ &+ g_2\sum_i\sum_{\sigma=-1}^{+1}\left(b_{i,\sigma} + b_{i,\sigma}^\dagger\right)\left(X_i^{s,\sigma} + X_i^{\sigma,s}\right)\end{aligned} \tag{17}$$

describes the off-diagonal electron–phonon processes corresponding to the transitions from the singlet $|s\rangle$ to triplet state $|\sigma\rangle$ and back. In Eqs. (16) and (17), $g_{1(2)}$ are the electron–phonon coupling constants and $\omega_{0(1,2)}$ are the frequencies of *a* and *b* type phonons.

3. TOY MODEL

The photoinduced enhancement of the exciton condensate in the one-dimensional two-band model of spinless fermions interacting with *a* and *b* type phonons was discussed in [13]. By solving the system of equations of motion for the operators of the electron and phonon subsystems and their averages in the time-dependent mean field approximation taking into account the external pumping, the authors of [13] demonstrated a new mechanism for the photoinduced enhancement of the excitonic order due to the arising massive mode (opening of a gap) in the spectrum of collective excitations and a change in the ground state under the effect of external radiation, which is not related to the excitation of metastable or any other states of the system lying higher in energy. In contrast to [13], where the Coulomb interaction is responsible for electron–hole pairing and the formation of excitons, in our case, the interactions J_{ex}' and J_{ex}'' in the Hamiltonian (13) are of a kinematic nature and are due to electron hopping between crystal lattice sites, but the photoinduced enhancement mechanism [13] can also be implemented in this case. However, solving the system of equations of motion for the Hubbard *X* operators with the Hamiltonian (15) is a rather cumbersome task. Let us try to simplify the case considered above as much as possible and analyze the mechanism of photoinduced enhancement based by the example of an artificially simplified Hamiltonian of a two-level system of local one-electron states 0 and 1 with the energies ε_0 and ε_1, respectively. To do this, instead of Eq. (13), we use the Hamiltonian

$$\begin{aligned}\hat{H}_{\text{ex}} &= \varepsilon_0\sum_i c_{0i}^\dagger c_{0i} + \varepsilon_1\sum_i c_{1i}^\dagger c_{1i}\\ &+ \frac{J_{\text{ex}}'}{2}\sum_{\langle i,j\rangle}\left(c_{0i}^\dagger c_{1i}c_{1j}^\dagger c_{0j} + c_{1i}^\dagger c_{0i}c_{0j}^\dagger c_{1j}\right)\\ &+ \frac{J_{\text{ex}}''}{2}\sum_{\langle i,j\rangle}\left(c_{1i}^\dagger c_{0i}c_{1j}^\dagger c_{0j} + c_{0i}^\dagger c_{1i}c_{0j}^\dagger c_{1j}\right),\end{aligned} \tag{18}$$

which is similar in its meaning, but is written in the representation of single-particle Fermi spinless annihilation (creation) operators $c_{\lambda i}$ ($c_{\lambda i}^\dagger$) of electrons at the *i*th site in the states $\lambda = 0$ and 1. In particular, the operator product $c_{1i}^\dagger c_{0i}$ in Eq. (18) describes the transition from the two-particle singlet $|s\rangle$ state to the triplet $|\sigma\rangle$ one, as the operator $X_i^{\sigma,s}$ in Eq. (13).

Taking into account the electron–phonon interaction, we have

$$\hat{H} = \hat{H}_{\text{ex}} + \hat{H}_{1\text{ph}} + \hat{H}_{2\text{ph}}, \tag{19}$$

where

$$\begin{aligned}\hat{H}_{1\text{ph}} &= \hbar\omega_{0(1)}\sum_i\left(a_i^\dagger a_i + \frac{1}{2}\right)\\ &+ g_1\sum_i\left(a_i + a_i^\dagger\right)\left(c_{0i}^\dagger c_{0i} - c_{1i}^\dagger c_{1i}\right)\end{aligned} \tag{20}$$

in much the same way as (16) contains the diagonal electron–phonon interaction, whereas

$$\begin{aligned}\hat{H}_{2\text{ph}} &= \hbar\omega_{0(2)}\sum_i\left(b_i^\dagger b_i + \frac{1}{2}\right)\\ &+ g_2\sum_i\left(b_i + b_i^\dagger\right)\left(c_{1i}^\dagger c_{0i} + c_{0i}^\dagger c_{1i}\right)\end{aligned} \tag{21}$$

in much the same was as (17) describes the off-diagonal transitions from state 0 to state 1 and back induced by the electron–phonon interaction.

In the mean field (MF) approximation, the Hamiltonian (18) has the form

$$\begin{aligned}\hat{H}_{\text{ex}}^{\text{MF}} &= \varepsilon_0\sum_i c_{0i}^\dagger c_{0i} + \varepsilon_1\sum_i c_{1i}^\dagger c_{1i}\\ &+ \sum_i\left[\left(zJ_{\text{ex}}'\phi + zJ_{\text{ex}}''\phi^*\right)c_{1i}^\dagger c_{0i}\right.\\ &\left.+ \left(zJ_{\text{ex}}'\phi^* + zJ_{\text{ex}}''\phi\right)c_{0i}^\dagger c_{1i}\right]\\ &- zJ_{\text{ex}}'N\phi\phi^* - z\frac{J_{\text{ex}}''}{2}N\left(\phi\phi + \phi^*\phi^*\right),\end{aligned} \tag{22}$$

where $\phi = \langle \hat{\phi}_i \rangle \equiv \langle c_{0i}^{\dagger} c_{1i} \rangle$ is the excitonic order parameter similar to $\Delta_{ex}^{\sigma} = \langle X_i^{s,\sigma} \rangle$ in the case of Eq. (13) and N is the number of the crystal lattice sites.

By solving the self-consistent eigenvalue problem

$$\hat{H}_{MF} |i,m\rangle = E_m |i,m\rangle, \tag{23}$$

where $|i,m\rangle$ ($m = 0,1,\ldots,\mathcal{N}$) are the eigenstates of the Hamiltonian $\hat{H}_{MF} = \hat{H}_{ex}^{MF} + \hat{H}_{1ph} + \hat{H}_{2ph}$, we can find the averages of interest

$$\phi = \frac{1}{Z} \sum_m \langle i,m | \hat{\phi}_i | i,m \rangle e^{-E_m/k_B T}, \tag{24}$$

corresponding to the global minimum of the free energy $F = -k_B T \ln Z$, where $Z = \sum_m e^{-E_m/k_B T}$ is the partition function of the system at different values of the spin gap $\varepsilon_S = \varepsilon_1 - \varepsilon_0$ (or of the applied pressure P) and the temperature T. Solutions (23) and (24), corresponding to the local minima of the free energy F, are metastable.

In Fig. 1, we present the dependence of ϕ on the splitting ε_S obtained in the mean field approximation at $T = 0$ (red dashed line) disregarding the electron–phonon interaction and (blue solid line) at $g_2 = 1.25J$ and $g_1 = 0$. We can see that the off-diagonal electron–phonon interaction expands the region of existence of excitons. On the contrary, at $g_2 = 0$ and $g_1 = 1.25J$ (the green solid line in Fig. 1), the range of exitonic ordering becomes narrower.

4. EXCITATION SPECTRUM

To determine the spectrum of excitonic excitations including collective ones in the exciton condensate phase ($\phi \neq 0$ in Fig. 1) and quasiparticle (single-particle) ones beyond the excitonic order range ($\phi = 0$ in Fig. 1), we use the generalized spin-wave approach. Below, we give a brief description of this approach. More details can be found in [14, 37, 38].

In terms of the operator $\hat{\phi}_i \equiv c_{0i}^{\dagger} c_{1i}$, the last two terms in (18) can be represented in the form similar to (14)

$$\begin{aligned} &\frac{J'_{ex}}{2} \sum_{\langle i,j \rangle} \left(\hat{\boldsymbol{\phi}}_i^{\dagger} \cdot \hat{\boldsymbol{\phi}}_j + \hat{\boldsymbol{\phi}}_i \cdot \hat{\boldsymbol{\phi}}_j^{\dagger} \right) \\ &+ \frac{J''_{ex}}{2} \sum_{\langle i,j \rangle} \left(\hat{\boldsymbol{\phi}}_i \cdot \hat{\boldsymbol{\phi}}_j + \hat{\boldsymbol{\phi}}_i^{\dagger} \cdot \hat{\boldsymbol{\phi}}_j^{\dagger} \right). \end{aligned} \tag{25}$$

The Hamiltonian (19) can be written as

$$\hat{H} = \hat{H}_{MF} + \delta \hat{H}_{ex}, \tag{26}$$

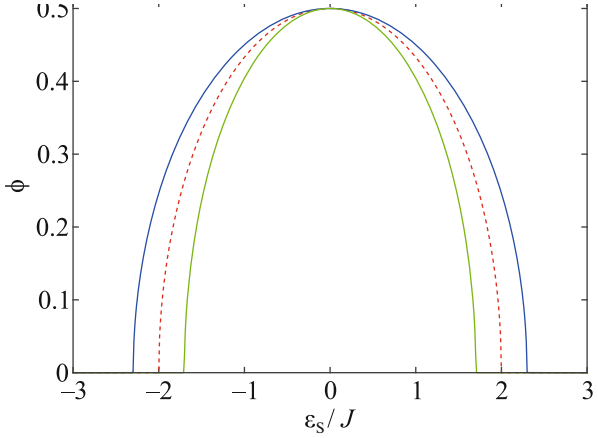

Fig. 1. (Color online) Excitonic order parameter ϕ versus the splitting ε_S calculated using the mean field approximation at $T = 0$, $z = 4$, $J = 28$ K, and $J''_{ex} = -0.5J$ (red dashed line) disregarding the electron–phonon interaction (i.e., $g_1 = g_2 = 0$), (blue solid line) taking into account the off-diagonal electron–phonon interaction ($g_1 = 0$, $g_2 = 1.25J$), and (green solid line) taking into account the diagonal electron–phonon interaction ($g_1 = 1.25J$, $g_2 = 0$).

where

$$\begin{aligned} \delta \hat{H}_{ex} = &\frac{1}{2} J'_{ex} \sum_{\langle i,j \rangle} \left(\delta \hat{\boldsymbol{\phi}}_i \cdot \delta \hat{\boldsymbol{\phi}}_j^{\dagger} + \delta \hat{\boldsymbol{\phi}}_i^{\dagger} \cdot \delta \hat{\boldsymbol{\phi}}_j \right) \\ &+ \frac{1}{2} J''_{ex} \sum_{\langle i,j \rangle} \left(\delta \hat{\boldsymbol{\phi}}_i \cdot \delta \hat{\boldsymbol{\phi}}_j + \delta \hat{\boldsymbol{\phi}}_i^{\dagger} \cdot \delta \hat{\boldsymbol{\phi}}_j^{\dagger} \right) \end{aligned} \tag{27}$$

describes the interactions beyond the mean field approximation, $\delta \hat{\phi}_i = \hat{\phi}_i - \langle \hat{\phi} \rangle_{MF}$.

The local fluctuation $\delta \hat{\phi}_i$ can be expanded in terms of the Hubbard X operators constructed on the eigenstates of the Hamiltonian $\hat{H}_{MF}$, which are determined by the solutions of the self-consistent eigenvalue problem given by Eqs. (23) and (24). Thus, we find

$$\delta \hat{\phi}_i = \sum_{m,n} \langle i,m | \delta \hat{\phi}_i | i,n \rangle X_i^{m,n} = \sum_{m,n} \gamma(m,n) X_i^{m,n}, \tag{28}$$

where $X_i^{m,n} = |i,m\rangle \langle n,i|$.

In the generalized Holstein–Primakoff representation, we have

$$X_i^{m,0} = h_{im}^{\dagger} \left(1 - \sum_{n=1}^{\mathcal{N}} h_{in}^{\dagger} h_{in} \right)^{1/2} \tag{29}$$

and $X_i^{0,m} = \left(X_i^{m,0} \right)^{\dagger}$ for $m \geq 1$,

$$X_i^{m,n} = h_{im}^{\dagger} h_{in} \tag{30}$$

for $m, n \geq 1$, and

$$X_i^{0,0} = 1 - \sum_{n=1}^{\mathcal{N}} h_{in}^{\dagger} h_{in}, \tag{31}$$

where $h_{in}^{\dagger}$ (h_{in}) are the Bose creation (annihilation) operators in the Holstein–Primakoff representation. Expression (31) follows from the condition $1 \equiv X_i^{0,0} + \sum_{n=1}^{\mathcal{N}} h_{in}^{\dagger} h_{in}$. Performing the series expansion of (29) and using the low-temperature relations $\left\langle i,0\left|\delta\hat{\phi}_i\right|i,0\right\rangle = \left\langle i,0\left|\hat{\phi}_i\right|i,0\right\rangle - \left\langle\hat{\phi}\right\rangle_{\mathrm{MF}} \approx 0$ or $\gamma(0,0) \approx 0$, we can represent the Hamiltonian (26) as a quadratic form omitting the terms of the orders exceeding two

$$\begin{aligned}\hat{H}_{\mathrm{SW}} &= \sum_{\mathbf{q},m\geq 1} \Delta E_m h_{\mathbf{q}m}^{\dagger} h_{\mathbf{q}m} \\ &+ \sum_{\mathbf{q},m\geq,n\geq 1,} \gamma_{\mathbf{q}} \left\{ J_{mn} h_{\mathbf{q}m}^{\dagger} h_{-\mathbf{q}n}^{\dagger} + \tilde{J}_{mn} h_{\mathbf{q}m}^{\dagger} h_{\mathbf{q}n} + \mathrm{h.c.} \right\},\end{aligned} \tag{32}$$

where $\Delta E_m = E_m - E_0$, $\gamma_{\mathbf{q}} = \sum_{\boldsymbol{\rho}} e^{i\mathbf{q}\cdot\boldsymbol{\rho}}$ (vector $\boldsymbol{\rho}$ runs over all nearest neighbors), $h_{\mathbf{q}m} = \frac{1}{\sqrt{N}} \sum_i e^{-i\mathbf{q}\cdot\mathbf{r}_i} h_{im}$,

$$\begin{aligned} J_{mn} &= \frac{J_{\mathrm{ex}}'}{2} \left\{ \gamma^*(0,m)\gamma(n,0) + \gamma(m,0)\gamma^*(0,n) \right\} \\ &+ \frac{J_{\mathrm{ex}}''}{2} \left\{ \gamma(m,0)\gamma(n,0) + \gamma^*(0,m)\gamma^*(0,n) \right\}, \\ \tilde{J}_{mn} &= \frac{J_{\mathrm{ex}}'}{2} \left\{ \gamma^*(0,m)\gamma(0,n) + \gamma(m,0)\gamma^*(n,0) \right\} \\ &+ \frac{J_{\mathrm{ex}}''}{2} \left\{ \gamma(m,0)\gamma(0,n) + \gamma^*(0,m)\gamma^*(n,0) \right\}. \end{aligned} \tag{33}$$

Using the paraunitary transformation [39], we can represent the Hamiltonian (32) in the diagonal form

$$\hat{H}_{\mathrm{SW}} = \sum_{\mathbf{q},\mu} \omega_{\mathbf{q}\mu} \alpha_{\mathbf{q}\mu}^{\dagger} \alpha_{\mathbf{q}\mu} + \mathrm{const}. \tag{34}$$

The generalized spin-wave approach allows us to determine the ac susceptibility. In our case, it is convenient to introduce the pseudospin $\hat{\mathbf{P}}$ with the components $\hat{P}_x = \hat{\phi} + \hat{\phi}^{\dagger}$ and $\hat{P}_y = i\left(\hat{\phi} - \hat{\phi}^{\dagger}\right)$ to the Hamiltonian (19) and to define the corresponding pseudospin susceptibility. At $T = 0$, the ac pseudospin susceptibility has the form

$$\begin{aligned}\chi_{\xi\xi'}(\mathbf{q},\omega) &= i\int_0^{\infty} dt \left\langle 0\left|\left[\delta\hat{P}_{\mathbf{q}\xi}(t), \delta\hat{P}_{-\mathbf{q}\xi'}\right]\right|0\right\rangle e^{i\omega t - \delta t} \\ &= -\int_{-\infty}^{\infty} dE \frac{A_{\xi\xi'}(\mathbf{q},E)}{\omega - E + i\delta},\end{aligned} \tag{35}$$

where $|0\rangle$ is the vacuum state for the operators $\alpha_{\mathbf{q}\mu}$ and $A_{\xi\xi'}(\mathbf{q},E)$ is the spectral function describing the spectral weight distribution for the collective excitations over the Brillouin zone

$$A_{\xi\xi'}(\mathbf{q},E) = -\frac{1}{\pi} \sum_{\mu} W_{\mathbf{q}\xi\mu} W_{\mathbf{q}\xi',\mu}^{*} \,\mathrm{Im}\left(\frac{1}{E - \omega_{\mathbf{q}\mu} + i\delta}\right), \tag{36}$$

where $W_{\mathbf{q}\xi\mu} = \sum_{\mathbf{q}'} \left\langle 0\left|\delta\hat{P}_{\mathbf{q}\xi}\right|\mu,\mathbf{q}'\right\rangle \left\langle\mu,\mathbf{q}'\left|\delta\hat{P}_{-\mathbf{q}\xi'}\right|0\right\rangle$, $|\mu,\mathbf{q}\rangle = \alpha_{\mathbf{q}\mu}^{\dagger}|0\rangle$.

In Fig. 2, the dispersion law $\omega_{\mathbf{q}\mu}$ is plotted by the dashed lines, and the colors illustrate the distribution of the total spectral weight $A(\mathbf{q},E) = A_{xx}(\mathbf{q},E) + A_{yy}(\mathbf{q},E)$. In Figs. 2a–2c, we present the results in the absence of electron–phonon interaction (a) in the exciton condensate phase and (b, c) outside it. Everywhere outside the exciton condensate phase, the spectrum has a gap (Figs. 2b and 2c), which vanishes at the onset of the second-order phase transition. This is consistent with the general idea that a gapless Goldstone mode should appear below the phase transition point (Fig. 2a) describing collective excitations in the exciton condensate phase. The spectrum in Figs. 2b and 2c describes collective excitations in the electron (Fermi) system, but it can be treated as a spectrum of quasiparticle (single-particle) excitations of a system of Bose particles described by the effective Hamiltonian (18). The formation of the gapless Goldstone mode (Fig. 2a) is preceded by closing of the gap in the quasiparticle spectrum of excitonic excitations (Figs. 2b, 2c).

The diagonal electron–phonon interaction g_1 does not change the spectrum qualitatively. On the contrary, the off-diagonal electron–phonon interaction g_2 (in Figs. 2d–2f, we show the calculation results in the presence of only the off-diagonal interaction ($g_2 = 1.25J$) (d) within the excitonic order range and (e, f) outside it) leads to the gap opening in the spectrum of collective excitations (Fig. 2d). In this case, the Bose spectrum of excitations—single-particle excitonic excitations (Figs. 2e and 2f) and collective ones in the excitonic phase (Fig. 2d)—exhibits a gap on both sides of the phase transition point. In [40], we calculated the spectrum of individual (single-particle) excitations using the method of two-time temperature Green's functions, and it is in excellent agreement with the spectrum obtained in this work by the generalized spin-wave approach.

As shown below, the gap in the spectrum of collective and single-particle excitations plays the key role in the photoinduced formation and enhancement of the excitonic order.

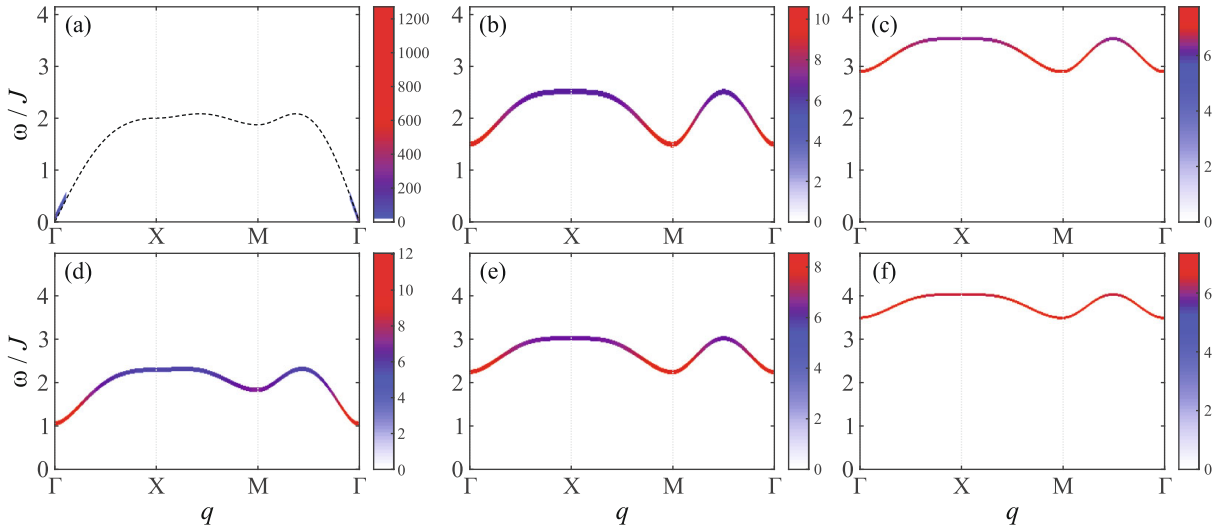

Fig. 2. (Color online) Excitation spectrum calculated with the parameters $z = 4$, $J = 28$ K, and $J''_{ex} = -0.5J$ (a–c) in the absence of the electron–phonon interaction (a) in the exciton condensate phase at $\varepsilon_S/J = 1.5$ and (b, c) outside the exciton condensate phase at $\varepsilon_S/J =$ (b) 2.5 and (c) 3.5 and (d–f) at nonzero off-diagonal electron–phonon interaction ($g_1 = 0$, $g_2 = 1.25J$) (d) within the excitonic order range at $\varepsilon_S/J = 2$ and (e, f) outside the excitonic order range at $\varepsilon_S/J =$ (e) 3 and (f) 4. The color palette illustrates the spectral weight distribution.

5. PHOTOINDUCED ENHANCEMENT

Let us supplement Eq. (19) with the term describing the interaction with external radiation

$$\hat{H}(t) = \hat{H} + \hat{V}(t), \tag{37}$$

where

$$\hat{V}(t) = E(t)\sum_i \left(c^\dagger_{1i\gamma}c_{0i\gamma} + c^\dagger_{0i\gamma}c_{1i\gamma}\right). \tag{38}$$

Here, we specify the applied field $E(t)$ in the form of wave train $E(t) = E_0 \sin(\Omega t)\exp\left[-(t-t_p)^2/\left(2\sigma_p^2\right)\right]$ with $\Omega = 6\tau_0^{-1}$, $\sigma_p = 3\tau_0$, $t_p = 25\tau_0$, and $E_0 = 0.15J$, where $\tau_0 = 10^{-12}$ s.

To obtain the closed set of equations of motion for the excitonic order parameter, we use the decoupling corresponding to the mean field approximation in the equation $\dot{\phi}_i = -i\left\langle\left[\hat{\phi}_i, \hat{H}(t)\right]\right\rangle$. In other words, in Eq. (37), we use Eq. (22) with the time-dependent excitonic order parameter $\phi(t)$ (time-dependent mean field approximation) instead of Eq. (18). In addition, we use the approximation $\left(b_i^\dagger + b_i\right)\left(c^\dagger_{i,1}c_{i,0} + c^\dagger_{i,0}c_{i,1}\right) \to X(t)\left(c^\dagger_{i,1}c_{i,0} + c^\dagger_{i,0}c_{i,1}\right) + 2\,\mathrm{Re}\,\phi(t)\left(b_i^\dagger + b_i\right)$ [13], where $X(t) = \left\langle b_i^\dagger + b_i\right\rangle$. With such a decoupling of the equations of motion, information about the spectrum of collective excitations becomes lost (Fig. 2). To take into account collective excitations, we supplement the Hamiltonian (22) with a small intersite hopping $\sum_{\langle i,j\rangle,\lambda=0,1} t_\lambda c^\dagger_{\lambda i}c_{\lambda j}$ ($t_\lambda = (-1)^{\lambda+1}\,0.07J$). Then, in the wave vector representation, we have

$$\dot{\phi}_{\mathbf{q}}(t) = -i\varepsilon_S(q)\phi_{\mathbf{q}}(t) - i\left\{zJ'_{ex}\phi(t) + zJ''_{ex}\phi^*(t) + g_2X(t) + E(t)\right\}\Delta n_{\mathbf{q}}(t); \tag{39}$$

$$\Delta\dot{n}_{\mathbf{q}}(t) = 4zJ'_{ex}\left[\mathrm{Re}\,\phi(t)\,\mathrm{Im}\,\phi_{\mathbf{q}}(t) - \mathrm{Re}\,\phi_{\mathbf{q}}(t)\,\mathrm{Im}\,\phi(t)\right] + 4zJ''_{ex}\left[\mathrm{Re}\,\phi(t)\,\mathrm{Im}\,\phi_{\mathbf{q}}(t) + \mathrm{Re}\,\phi_{\mathbf{q}}(t)\,\mathrm{Im}\,\phi(t)\right] + 4\left[g_2X(t) + E(t)\right]\mathrm{Im}\,\phi_{\mathbf{q}}; \tag{40}$$

$$\ddot{X}(t) = -\omega^2_{0(2)}X(t) - 2g_2\omega_{0(2)}\left[\phi(t) + \phi^*(t)\right], \tag{41}$$

where $\Delta n_{\mathbf{q}}(t) \equiv \left\langle c^\dagger_{0\mathbf{q}}c_{0\mathbf{q}}\right\rangle - \left\langle c^\dagger_{1\mathbf{q}}c_{1\mathbf{q}}\right\rangle$, $\phi_{\mathbf{q}}(t) \equiv \left\langle c^\dagger_{0\mathbf{q}}c_{1\mathbf{q}}\right\rangle$, $\phi(t) = \frac{1}{N}\sum_{\mathbf{q}}\phi_{\mathbf{q}}(t)$, and $\varepsilon_S(\mathbf{q}) \equiv (t_{1\mathbf{q}} - t_{0\mathbf{q}}) + \varepsilon_S$.

In Fig. 3, we show the results of solving the set of equations (39)–(41) for $g_2 =$ (a, c, e) 0 and (b, d, f) $1.25J$. Far outside the exciton range (Figs. 3e and 3f), after turning off the external radiation, the system returns to the initial state of thermal equilibrium, shown by the dashed line in all panels. Close to the exciton range (Figs. 3c and 3d), after turning off the external field, the order parameter exhibits temporal oscillations about the average value, denoted by the red solid line in all panels. This average value is different from that corresponding to the equilibrium one and exceeds it (photoinduced excitonic order). Finally, within the exciton range (Figs. 3a and 3b), we observe two opposite results: in the absence of elec-

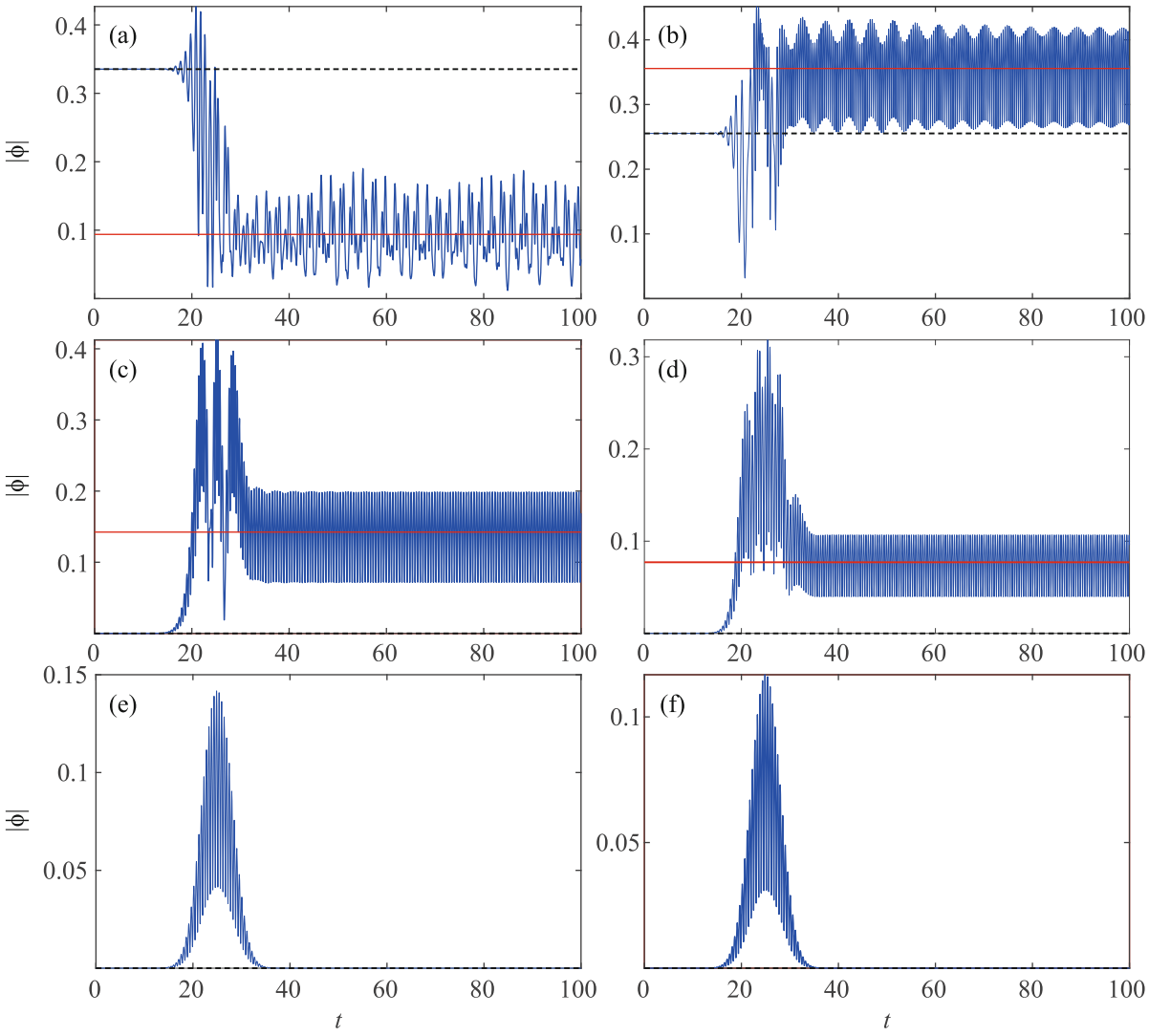

Fig. 3. (Color online) Time dependence of the excitonic order parameter $|\phi|$ after exposure to an external radiation pulse calculated with the parameters $z = 4$, $J = 28$ K, and $J''_{ex} = -0.5J$ (a, c, e) in the absence of the electron–phonon interaction at $\varepsilon_S/J =$ (a) 1.5, (c) 2.5, and 3.5 (e) and (b, d, f) at nonzero off-diagonal electron–phonon interaction ($g_2 = 1.25J$) at $\varepsilon_S/J =$ (b) 2, (d) 3, and (f) 4. The initial state of thermal equilibrium is indicated by the dashed line. The red solid line denotes the average value about which the order parameter oscillates after turning off the external radiation. The time t is measured in units of $\tau_0 = 10^{-12}$ s.

tron–phonon interaction (Fig. 3a), the order parameter decreases, while the photoinduced enhancement of the exciton condensate occurs at $g_2 = 1.25J$ (Fig. 3b). The observed behavior can be understood in terms of the collective excitation spectrum (Fig. 2). At $g_2 = 0$ in the excitonic phase (Fig. 3a), the emerging massless Goldstone modes result in a gapless energy spectrum of the system (Fig. 2a); hence, any small external perturbation leads to the excitation of collective modes and to a decrease in the order parameter (Fig. 3a). In the absence of relaxation and dissipative processes in the equations of motion (39)–(41), the system remains in the excited state after turning off the pumping. At $g_2 = 1.25J$ in the excitonic phase (Fig. 3b), a gap opens in the excitation spectrum (Fig. 2d), and the excitation of collective modes is complicated in this case. External radiation changes the ground state, so that it becomes time dependent and mixing of states 0 and 1 increases. Outside the exciton range, in both Figs. 3c and 3d, a gap in the spectrum of already individual excitonic excitations also appears (Figs. 2b, 2e), so we observe the photoinduced formation of the exciton condensate (Figs. 3c, 3d). Far outside the excitonic phase (at large ε_S/J, Figs. 3e and 3f), the energy barrier between the states 0 and 1 becomes insurmountably high, and the photoinduced formation of exciton condensate becomes impossible.

As mentioned above, a rather strong interplay occurs between the excitonic and magnetic orders [35], so a change in the exciton condensate will inevitably induce a response in the magnetic subsystem.

We believe that our work will stimulate further experimental studies of strongly correlated systems with the spin crossover using modern methods of pump–probe spectroscopy with a high time resolution.

FUNDING

This work was supported jointly by the Russian Science Foundation and the Krasnoyarsk Regional Science Foundation (project no. 22-22-20007).

CONFLICT OF INTEREST

The authors declare that they have no conflicts of interest.

REFERENCES

1. D. Fausti, R. I. Tobey, N. Dean, S. Kaiser, A. Dienst, M. C. Hoffmann, S. Pyon, T. Takayama, H. Takagi, and A. Cavalleri, Science (Washington, DC, U. S.) **331** (6014), 189 (2011).
2. S. Kaiser, C. R. Hunt, D. Nicoletti, W. Hu, I. Gierz, H. Y. Liu, M. Le Tacon, T. Loew, D. Haug, B. Keimer, and A. Cavalleri, Phys. Rev. B **89**, 184516 (2014).
3. M. Mitrano, A. Cantaluppi, D. Nicoletti, S. Kaiser, A. Perucchi, S. Lupi, P. di Pietro, D. Pontiroli, M. Riccò, S. Clark, D. Jaksch, and A. Cavalleri, Nature (London, U.K.) **530**, 461 (2016).
4. R. Matsunaga, Y. I. Hamada, K. Makise, Y. Uzawa, H. Terai, Z. Wang, and R. Shimano, Phys. Rev. Lett. **111**, 057002 (2013).
5. R. Matsunaga, N. Tsuji, H. Fujita, A. Sugioka, K. Makise, Y. Uzawa, H. Terai, Z. Wang, H. Aoki, and R. Shimano, Science (Washington, DC, U. S.) **345** (6201), 1145 (2014).
6. R. Matsunaga, N. Tsuji, K. Makise, H. Terai, H. Aoki, and R. Shimano, Phys. Rev. B **96**, 020505 (2017).
7. T. Rohwer, S. Hellmann, M. Wiesenmayer, C. Sohrt, A. Stange, B. Slomski, A. Carr, Y. Liu, L. M. Avila, M. Kallane, S. Mathias, L. Kipp, K. Rossnagel, and M. Bauer, Nature (London, U.K.) **471**, 490 (2011).
8. S. Hellmann, T. Rohwer, M. Kallane, K. Hanff, C. Sohrt, A. Stange, A. Carr, M. Murnane, H. Kapteyn, L. Kipp, M. Bauer, and K. Rossnagel, Nat. Commun. **3**, 1069 (2012).
9. M. Porer, U. Leierseder, J.-M. Menard, H. Dachraoui, L. Mouchliadis, I. E. Perakis, U. Heinzmann, J. Demsar, K. Rossnagel, and R. Huber, Nat. Mater. **13**, 857 (2014).
10. D. Golež, P. Werner, and M. Eckstein, Phys. Rev. B **94**, 035121 (2016).
11. S. Mor, M. Herzog, D. Golež, P. Werner, M. Eckstein, N. Katayama, M. Nohara, H. Takagi, T. Mizokawa, C. Monney, and J. Stähler, Phys. Rev. Lett. **119**, 086401 (2017).
12. D. Werdehausen, T. Takayama, M. Hoppner, G. Albrecht, A. W. Rost, Y. Lu, D. Manske, H. Takagi, and S. Kaiser, Sci. Adv. **4**, eaap8652 (2018).
13. Y. Murakami, D. Golež, M. Eckstein, and P. Werner, Phys. Rev. Lett. **119**, 247601 (2017).
14. J. Nasu, T. Watanabe, M. Naka, and S. Ishihara, Phys. Rev. B **93**, 205136 (2016).
15. J. Kuneš, J. Phys.: Condens. Matter **27**, 333201 (2015).
16. P. Werner and A. J. Millis, Phys. Rev. Lett. **99**, 126405 (2007).
17. R. Suzuki, T. Watanabe, and S. Ishihara, Phys. Rev. B **80**, 054410 (2009).
18. L. Balents, Phys. Rev. B **62**, 2346 (2000).
19. T. Kaneko and Y. Ohta, Phys. Rev. B **90**, 245144 (2014).
20. J. Kuneš and P. Augustinský, Phys. Rev. B **89**, 115134 (2014).
21. A. Sotnikov and J. Kuneš, Sci. Rep. **6**, 30510 (2016).
22. T. Tatsuno, E. Mizoguchi, J. Nasu, M. Naka, and S. Ishihara, J. Phys. Soc. Jpn. **85**, 083706 (2016).
23. G. Khaliullin, Phys. Rev. Lett. **111**, 197201 (2013)).
24. A. Ikeda, Y. H. Matsuda, K. Sato, Y. Ishii, H. Sawabe, D. Nakamura, S. Takeyama, and J. Nasu, Nat. Commun. **14**, 1744 (2023).
25. S. Londo, S. Biswas, I. V. Pinchuk, A. Boyadzhiev, R. K. Kawakami, and L. R. Baker, J. Phys. Chem. C **126**, 2669 (2022).
26. T. K. Ekanayaka, K. P. Maity, B. Doudin, and P. A. Dowben, Nanomaterials **12**, 1742 (2022).
27. J. Kanamori, Prog. Theor. Phys. **30**, 275 (1963).
28. J. Hubbard, Proc. R. Soc. A **277** (1369), 237 (1964).
29. R. O. Zaitsev, Sov. Phys. JETP **43**, 574 (1976).
30. K. A. Chao, J. Spalek, and A. M. Oles, J. Phys. C **10**, L271 (1977).
31. V. A. Gavrichkov, S. I. Polukeev, and S. G. Ovchinnikov, Phys. Rev. B **95**, 144424 (2017).
32. V. V. Val'kov and S. G. Ovchinnikov, Theor. Math. Phys. **50**, 466 (1982).
33. S. V. Vonsovskii and M. S. Svirskii, Sov. Phys. JETP **20**, 914 (1965).
34. V. M. Agranovich and B. S. Toshich, Sov. Phys. JETP **26**, 104 (1968).
35. Y. S. Orlov, S. V. Nikolaev, and S. G. Ovchinnikov, JETP Lett. **117**, 708 (2023).
36. M. J. R. Hoch, S. Nellutla, J. van Tol, E. S. Choi, J. Lu, H. Zheng, and J. F. Mitchell, Phys. Rev. B **79**, 214421 (2009).
37. F. P. Onufrieva, Sov. Phys. JETP **62**, 1311 (1985).
38. J. Nasu and S. Ishihara, Phys. Rev. B **88**, 205110 (2013).
39. J. Colpa, Phys. A (Amsterdam, Neth.) **93**, 327 (1978).
40. Y. S. Orlov, S. V. Nikolaev, V. I. Kuz'min, A. E. Zarubin, and S. G. Ovchinnikov, Phys. Rev. B **106**, 235120 (2022).

Translated by K. Kugel